Ionization levels of As vacancies in as-grown GaAs studied by positron-lifetime spectroscopy

K. Saarinen, P. Hautojärvi, and P. Lanki
Laboratory of Physics, Helsinki University of Technology, 02150 Espoo, Finland

C. Corbel
Centre d'Etudes Nucléaires de Saclay, Institut National des Sciences et Techniques Nucléaires, 91191 Gif-sur-Yvette CEDEX, France

(Received 29 January 1991; revised manuscript received 18 June 1991)

The properties of the native monovacancy defects are systematically investigated by positron-lifetime measurements in n-type GaAs with carrier concentrations of $n=10^{15}$–10^{18} cm^{-3}. The native defects present two ionization levels at E_C-30 meV and E_C-140 meV. The first corresponds to a charge transition $1-\rightarrow 0$ and the second to $0\rightarrow 1+$. The transitions are attributed to ionizations of As vacancy, which may be isolated or part of a complex. In a simple identification of the defect with V_{As}, the ionization level at E_C-30 meV is attributed to the transition $V_{As}^{-}\rightarrow V_{As}^{0}$ and the ionization level at E_C-140 meV to the transition $V_{As}^{0}\rightarrow V_{As}^{+}$. The results show further that the configuration of V_{As}^{-} is strongly relaxed inwards compared to the structure of V_{As}^{0}.

I. INTRODUCTION

During the crystal growth of gallium arsenide, various defects are formed in the lattice. These defects interact with the free carriers by acting as traps, and scattering and recombination centers. Therefore, they have a strong influence on the electrical and optical properties of the semiconductor material. However, the microscopic structures of the defects in as-grown material are still largely unknown, and there is need for their direct characterization by atomic probes. In case of vacancies as native defects in GaAs, positron-annihilation methods have already proved to yield valuable information on the basic properties of the defects, like their charge state or ionization levels.[1–3]

Positrons in solids are strongly repelled by positive-ion cores. Open-volume defects act as attractive centers, at which positrons can get trapped with subsequent changes in their annihilation characteristics. Because the electron density in these defects is reduced compared to bulk, the lifetime of the trapped positron is larger than the lifetime of positrons annihilating in the perfect crystal. Consequently, positron-lifetime experiments can be used to obtain direct information on the vacancy-type defects on an atomic scale.[4,5] In addition to vacancies, also negative ions have recently been shown to trap positrons at Rydberg states at low temperatures both in as-grown and electron-irradiated GaAs.[6–9]

We have used positron-lifetime experiments so far to characterize both the native vacancies and the defects created during 1–3-MeV electron irradiation in GaAs.[2,8,9] In as-grown n-type GaAs, positron trapping at native vacancies has been observed.[2] In our earlier study, we have suggested that these vacancies exhibit two Fermi-level-controlled transitions in the upper half of the energy gap, and we have interpreted these processes as ionizations of the As monovacancy.[2] This identification is further supported by our recent experiments in electron irradiated n-type GaAs, which clearly show that the native vacancies change their charge during the compensation of the material by irradiation.[8]

Our earlier results on the native vacancies in as-grown n-type GaAs were mostly based on positron-lifetime experiments performed as a function of temperature between 77 and 400 K in samples with a carrier concentration of typically $n\geq 10^{16}$ cm^{-3}.[2] The aim of this paper is to complete our previous work and to obtain more detailed information on the ionization processes. To observe the positron-lifetime transitions more completely in n-type GaAs crystals with carrier concentrations of about 10^{17}–10^{18} cm^{-3}, we extend the temperature range of our measurements up to 600 K. We also extend it down to 10 K to investigate nominally undoped GaAs crystals with carrier concentrations between 10^{15} and 10^{16} cm^{-3}. It is interesting to test whether the native vacancies in n-type GaAs exhibit the same properties as in our previous work,[2] when the expanded scales of temperature and carrier concentration are utilized in the experiments.

Our results show that the position of the Fermi level in the energy gap is able to explain the positron lifetimes at native vacancies in n-type GaAs samples with carrier concentrations ranging over three orders of magnitude from $n=10^{15}$ to 10^{18} cm^{-3}. Two ionization processes of monovacancy defects were found at E_C-30 meV and at E_C-140 meV after a careful data analysis, where the influences of the degeneracy factors and the changes in the positron-trapping coefficients are taken into account. The monovacancy defect is attributed to As vacancy, which may be isolated or bound to a defect complex. The ionizations at E_C-30 meV and at E_C-140 meV correspond to transitions of $1-\rightarrow 0$ and $0\rightarrow 1+$ in the total charge of the defect involving V_{AS}. If the total charge is attributed to As vacancy, our results show that V_{As}^{-} is strongly inwards relaxed compared to V_{As}^{0}.

II. EXPERIMENTAL DETAILS

Positron lifetimes were measured in n-type GaAs single crystals (see Table I), which were grown either by liquid-encapsulated Czochralski (LEC) or horizontal Bridgman (HB) method. The carrier concentrations of our samples were between $n=10^{15}-10^{18}$ cm^{-3} at 300 K, and Hall experiments were performed for several samples at 300 and 77 K to check the carrier concentrations given by the suppliers of the sample material. The crystals at $n=10^{15}-10^{16}$ cm^{-3} were intentionally undoped, and their electrical conductivity is most probably due to residual Si impurities. The samples with $n=10^{17}-10^{18}$ cm^{-3} were doped either with Si or Sn. In addition to n-type GaAs, positron lifetimes were measured also in three Zn-doped p-type samples with room-temperature carrier concentrations of 5.4×10^{16}, 6.2×10^{17}, and 2.0×10^{18} cm^{-3}, respectively. Before the positron experiments the samples were etched at $[H_2SO_4]:[H_2O_2]:[H_2O]$ 3:1:1 solution to remove a layer of about 10–20 μm from the surface.

The positron-lifetime experiments were performed in a conventional way.[4] Two identical sample pieces cut from the same wafer were sandwiched with a 10–20-μCi positron source. The source material was carrier-free ^{22}NaCl solution deposited onto a thin (1 μm) nickel foil. Positron-lifetime measurements were carried out by a fast-fast lifetime spectrometer with a time resolution of 230 ps [full width at half maximum (FWHM)]. Roughly 2×10^6 counts were collected to each of the spectrum, and the annihilations in the source materials (145 ps, 7.4%; 450 ps, 2.0%) were subtracted from the spectra before the final analysis. A closed-cycle He cryocooler and a liquid-nitrogen cryostat were used to vary the sample temperature between 10 and 600 K.

After the source and background corrections, the lifetime spectra were fitted to a sum of two exponential components:

$$n(t)=n_0[I_1\exp(-\lambda_1 t)+I_2\exp(-\lambda_2 t)] , \quad (1)$$

convoluted with the Gaussian resolution function of the spectrometer. In Eq. (1), n_0 is the total number of observed annihilation events, and the annihilation rate λ_i is the inverse of the positron lifetime, $\lambda_i=\tau_i^{-1}$. I_i denotes the relative intensity of the component having the lifetime τ_i. The decomposition of the lifetime spectra is unambiguous when the lifetime values differ sufficiently, i.e., $\tau_2/\tau_1>1.5$. From the values of lifetimes τ_i and intensities I_i we calculated also the average lifetime

$$\tau_{\rm av}=I_1\tau_1+I_2\tau_2 , \quad (2)$$

which is insensitive to the uncertainties in the decomposition procedure and coincides with the center of mass of the spectrum. Hence, the average lifetime is always accurately known, even when the two-component analysis is not possible ($\tau_2/\tau_1<1.5$).

III. POSITRON-TRAPPING MODELS

In a perfect crystal, delocalized positrons annihilate with a single lifetime τ_b. In the presence of defects, positrons may get localized at them and annihilate with a second lifetime τ_d. For open-volume defects like vacancies, this lifetime is always longer than the bulk lifetime, because the electron density is lower in a vacancy defect. The positron trapping rate κ at defects is proportional to the defect concentration c_d, and it is given by

$$\kappa=\mu_d c_d , \quad (3)$$

where μ_d is the positron-trapping coefficient.

In semiconductors, the vacancy defects can exist in different charge states depending on the position of Fermi level in the energy gap. The charge of the vacancy has a large influence on the positron-trapping coefficient μ_d. For instance, positive vacancies are repulsive for positrons, whereas strongly enhanced positron trapping at negative vacancies is observed at low temperatures.[10,11] Furthermore, if the vacancy changes its open volume at the ionization process, the lifetime of the trapped positron τ_d can also be different at various charge states of the vacancy. To investigate quantitatively these charge transitions with positron-lifetime measurements, the standard positron-trapping model[12] has to be reformulated to take into account the various charge states of the defects. The models developed here will be used to analyze our experimental data in Sec. VI.

TABLE I. The n-type samples studied in this work and their positron-lifetime decompositions at room temperature. The n-type conductivity of the nominally undoped samples is most probably due to silicon impurities.

Carrier concentration (cm^{-3})	Dopant atom	$\tau_{\rm av}$ (ps)	τ_1 (ps)	τ_2 (ps)	I_2 (%)
1.9×10^{15}	undoped	238±1	208±11	290±11	38±11
4.6×10^{15}	undoped	248±1	199±11	287±8	56±11
2.5×10^{16}	undoped	263±1	112±6	289±2	86±2
6.2×10^{16}	Si	257±1	120±6	281±2	85±2
1.2×10^{17}	Sn	243±1	176±9	274±4	67±5
1.8×10^{17}	Si	240±1	173±13	263±4	73±8
2.0×10^{18}	Si	240±1	166±15	257±4	81±5

A. Positron trapping at vacancies with a single charge state

When only one type of vacancy defects with a single charge state exists in the sample, positrons can annihilate either as delocalized in the bulk or as trapped at the vacancy. Provided that a trapped positron does not escape from the vacancy, the lifetime spectrum is two exponential, and the normal one-defect trapping model is valid. The lifetimes and intensities are given by[12]

$$\tau_1^{-1}=\tau_b^{-1}+\kappa \ , \tag{4}$$

$$\tau_2=\tau_d \ , \tag{5}$$

$$I_2=1-I_1=\frac{\kappa}{\kappa+\lambda_b-\lambda_d} \ . \tag{6}$$

By applying Eqs. (4)–(6) to Eq. (2), the positron-trapping rate can be expressed in terms of the average lifetime as

$$\kappa=\lambda_b\frac{\tau_{\rm av}-\tau_b}{\tau_d-\tau_{\rm av}} \ . \tag{7}$$

This equation can be used to calculate the defect concentration $c_d=\kappa/\mu_d$, if the trapping coefficient μ_d is known. The consistency of the one-defect trapping model can be checked from the following equation:

$$1/\tau_0=I_1/\tau_1+I_2/\tau_2=1/\tau_b \ . \tag{8}$$

The test parameter τ_0 in Eq. (8) should coincide with the known value of bulk lifetime τ_b, if the decomposition (τ_i,I_i) follows the one-defect trapping model. If there is a significant difference ($\tau_0-\tau_b>5$ ps), more than one type of positron traps exist in the sample.

B. Positron trapping at vacancies with two different charge states

When a vacancy defect has an ionization level in the energy gap, two different charge states are possible for the vacancy. The total vacancy concentration c consists thus of two populations c_A and c_B, which can change into each other by the ionization reaction $c_A\leftrightarrow c_B+e^-$. Positrons can then get trapped either at the vacancies of type A or B, and the annihilation characteristics in these two states might be different. The occupancy of the vacancy between the two states A and B is determined by the Fermi function f (Ref. 13):

$$c_A=fc=\kappa_A/\mu_A \ , \tag{9}$$

$$c_B=(1-f)c=\kappa_B/\mu_B \ , \tag{10}$$

where κ_A, μ_A, κ_B, and μ_B are the positron trapping rates and trapping coefficients to the vacancy states A and B, respectively. The Fermi distribution function f at the temperature T can be written as

$$f=\{1+g\exp[(E_i-E_F)/k_BT]\}^{-1} \ . \tag{11}$$

E_i is the ionization level of the vacancy and E_F is the Fermi level. The factor g is the ratio $g=Z_B/Z_A$ of the internal degeneracies Z_A and Z_B of the states A and B, respectively.

At the charge transition $A\leftrightarrow B$, the positron-annihilation characteristics can change in two ways. First, the lifetime of the trapped positron might change due to differences in the electron density or in the volume relaxation between the states A and B. Second, the trapping coefficient can depend strongly on the charge of the vacancy, even if the positron lifetime remains unaffected in the ionization process. In next sections, we shall discuss these two possible effects on the basis of the positron-trapping model.

1. *Transition of positron lifetime in the ionization of vacancy*

When the lifetime of the trapping positron changes with the charge state of the vacancy, the lifetime spectrum at the transition is three componential. In a three-state trapping model the positron lifetimes $\tau_{\rm I}$, $\tau_{\rm II}$, and $\tau_{\rm III}$ are given by[12]

$$\tau_{\rm I}^{-1}=\tau_b^{-1}+\kappa_A+\kappa_B \ , \tag{12}$$

$$\tau_{\rm II}=\tau_A \ , \tag{13}$$

$$\tau_{\rm III}=\tau_B \ , \tag{14}$$

with the corresponding intensities

$$I_{\rm I}=1-I_{\rm II}-I_{\rm III} \ , \tag{15}$$

$$I_{\rm II}=\kappa_A/(\lambda_b-\lambda_A+\kappa_A+\kappa_B) \ , \tag{16}$$

$$I_{\rm III}=\kappa_B/(\lambda_b-\lambda_B+\kappa_A+\kappa_B) \ . \tag{17}$$

In practice, three-component analysis of positron-lifetime spectra is not possible due to statistical scattering, if the longer lifetimes $\tau_{\rm II}$ and $\tau_{\rm III}$ differ less than typically 100 ps. In a two-component analysis, the shortest lifetime $\tau_{\rm I}$ is usually well separated from the others, whereas the experimental second lifetime becomes a weighted sum of the longer lifetimes $\tau_{\rm II}$ and $\tau_{\rm III}$. The decomposition (τ_1,τ_2) becomes then

$$\tau_1=\tau_{\rm I} \ , \tag{18}$$

$$\tau_2=\frac{I_{\rm II}\tau_{\rm II}+I_{\rm III}\tau_{\rm III}}{I_{\rm II}+I_{\rm III}} \ . \tag{19}$$

According to Eq. (19), the experimental second lifetime τ_2 can thus be used to get information on the positron lifetimes τ_A and τ_B [see Eqs. (13) and (14)] at the two charge states A and B of the vacancy defect.

Equation (19) can be simplified in the limit of a large vacancy concentration. Assuming that $(\kappa_A+\kappa_B)$ is much larger than $(\lambda_b-\lambda_A)$ or $(\lambda_b-\lambda_B)$, a substitution of Eqs. (12)–(17) to Eq. (19) yields

$$\tau_2=\frac{\kappa_A}{\kappa_A+\kappa_B}\tau_A+\frac{\kappa_B}{\kappa_A+\kappa_B}\tau_B \ . \tag{20}$$

Using Eqs. (9)–(11) we get a model curve for τ_2 in the transition $A\leftrightarrow B$:

$$\tau_2=f_{e^+}\tau_A+(1-f_{e^+})\tau_B \ , \tag{21}$$

where f_{e^+} is the Fermi distribution of the vacancy charge states A and B as seen by the positron

$$f_{e^+}=\left[1+\frac{g}{\mu_{\text{eff}}}\exp[(E_i-E_F)/k_BT]\right]^{-1} . \quad (22)$$

The parameter μ_{eff} is the ratio of the positron-trapping coefficients to the vacancy states A and B, $\mu_{\text{eff}}=\mu_A/\mu_B$. When a transition $\tau_A \leftrightarrow \tau_B$ is observed in the lifetime of the trapped positron τ_2, Eq. (21) can be fitted to the experimental data to obtain the corresponding ionization level E_i.

2. *Transition of positron-trapping coefficient in the ionization of a vacancy*

When the lifetime of the trapped positron remains constant in the ionization of the vacancy, the only change to the lifetime spectrum is due to different positron-trapping coefficients at the two charge states A and B of the vacancy. In this case, the lifetime spectrum is two exponential with $\tau_2=\tau_A=\tau_B$. The total trapping rate κ can be calculated from the one-defect trapping model [Eq. (7)] with the experimental values of τ_{av} and τ_2:

$$\kappa=\kappa_A+\kappa_B=\lambda_b\frac{\tau_{\text{av}}-\tau_b}{\tau_2-\tau_{\text{av}}} . \quad (23)$$

Using Eqs. (9)–(12) we get, from Eq. (23),

$$\frac{\kappa}{\kappa_0}=f+\frac{\mu_B}{\mu_A}(1-f) , \quad (24)$$

where $\kappa_0=\mu_A c$, i.e., the trapping rate at vacancy state A when $f=1$. Equation (24) can be used to model the experimental data in order to obtain the ionization level E_i of the vacancy in the transition $A \leftrightarrow B$. Note that when μ_B is much smaller than μ_A, the measured values of κ describe directly the Fermi function f of the vacancy ionization process. This situation could be expected, when a vacancy changes its charge from neutral to positive.

IV. POSITRON LIFETIME RESULTS IN *p*-TYPE GaAs

In p-type GaAs, three different samples with carrier concentrations ranging from 5.4×10^{16} to 2×10^{18} cm^{-3} were studied as a function of temperature at 85–600 K. The results are shown in Fig. 1.

In p-type GaAs, the lifetime spectrum is one componential at all temperatures, and no signs of positron trapping were observed. As seen in Fig. 1, the positron lifetime increases as a function of temperature in all three samples. The value of 231 ps was obtained for all samples at 300 K, and the increase of the lifetime takes place with the same slope as a function of temperature independent of the carrier concentration of the sample. A linear fit to the experimental lifetime gives the result of $\tau=227.6$ ps$+(0.0113$ ps/K$)\,T$ for the temperature dependence of τ in Fig. 1.

In p-type GaAs, no positron trapping at vacancies is thus observed. The lifetime value of 231 ps is the lowest lifetime we have measured in GaAs at 300 K. This value

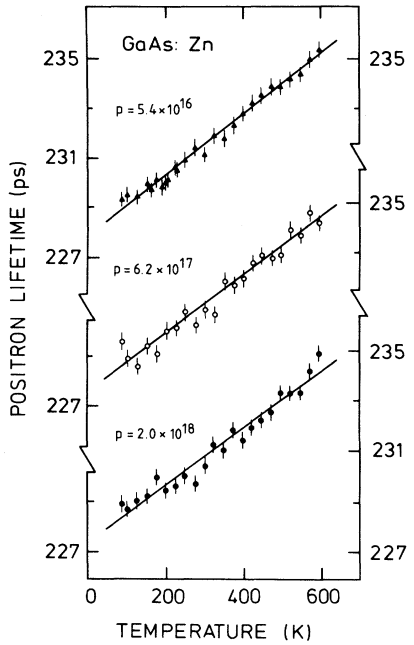

FIG. 1. Positron lifetimes in as a function of measurement temperature in p-type Zn-doped GaAs. The lifetime spectra in p-type GaAs are one componential. The carrier concentrations in cm^{-3} at 300 K are indicated for each sample in the figure.

can also be calculated from the one-defect trapping model [Eq. (8)], when positron traps are present in the material (Sec. V). Hence, we follow our previous conclusion[2] and attribute the lifetime of 231 ps to delocalized positrons in bulk GaAs. The bulk lifetime of 231 ps is in good agreement with the recent theoretical calculations.[14]

In defect-free materials, the temperature dependence of the positron lifetime is due to the thermal expansion of the lattice and to the positron-phonon interaction. This results at high temperatures to a smaller valence-electron density in the interstitial regions of the lattice, where the positron is confined. In Fig. 1, the temperature dependence of the bulk positron lifetime in GaAs crystal mainly reflects the thermal expansion of the lattice. We can check this by comparing the ratios of the positron-lifetime increase to the ratios of the standard linear thermal expansion coefficients of the lattice in different semiconductors. For instance, for GaAs and Si we get a ratio of about $(0.0113/0.0069)\approx2$ from our positron experiments, whereas a value of $(6.86\times10^{-6}\ \text{K}^{-1})/(2.6\times10^{-6}\ \text{K}^{-1})=2.6$ can be calculated from the thermal expansion coefficients.[15]

However, in p-type GaAs positrons are not necessarily completely free at low temperatures, since a weak localization at Rydberg states of negative ions like Zn atoms can occur.[6] If this process is possible in p-type GaAs, it is not visible at 85–600 K in the temperature dependence of positron lifetime according to data in Fig. 1. We can thus conclude that in p-type GaAs positrons do not detect vacancies and the temperature dependence of the positron lifetime is due to thermal expansion only.

V. POSITRON-LIFETIME RESULTS IN *n*-TYPE GaAs

A. Positron lifetimes at room temperature

In *n*-type GaAs, two exponential positron-decay components were necessary to analyze the lifetime spectra at room temperature. The results of the decompositions at room temperature are given in Table I for the samples with various *n*-type doping levels.

In Table I, both the average lifetime and the decomposition of the lifetime spectra depend on the carrier concentration at 300 K. In the samples with a low doping level of $10^{15}-10^{16}$ cm^{-3}, the average lifetime shows large variations between 238 and 263 ps, whereas in highly doped material ($n=10^{17}-10^{18}$ cm^{-3}) τ_{av} always gets values of about 240 ps. The average lifetime in lightly *n*-type GaAs is thus generally equal or larger than in highly *n*-type GaAs. This trend is in good accordance with the results of earlier experiments.[1-3]

As a function of the carrier concentration, the decompositions of the lifetime spectra show similar trends as the average lifetime. The lifetime component τ_2 is about 290 ps in the *n*-type samples with a small free-electron concentration of $10^{15}-10^{16}$ cm^{-3} at 300 K. When the carrier concentration is increased to the intermediate doping level of 10^{17} cm^{-3}, the positron-lifetime component τ_2 tends to decrease to values of 265–285 ps. Finally, in heavily *n*-type material the lifetime τ_2 gets the lowest values, typically at the level of 257–262 ps.

Positron average lifetime values of 240–270 ps are clearly higher than the lifetime $\tau_b=231$ ps of delocalized positrons in the bulk GaAs at 300 K. Increased value of average lifetime is a clear sign that the sample contains vacancy-type defects, at which positrons get trapped. Our results in Table I thus reproduce the general trend that vacancy-type defects are detected in *n* GaAs but not in *p* GaAs nor in semiinsulating GaAs. This behavior has also been found in earlier experiments.[1,2]

In the one-defect trapping model,[12] the experimental lifetime τ_2 is characteristic for positrons trapped at the corresponding vacancy defect (see Sec. III A). Using Eq. (8), the consistency of the one-defect trapping model can be checked by calculating the test parameter τ_0 from the lifetime decompositions and by comparing it to the lifetime τ_b obtained in defect-free GaAs. In our results in Table I, the mean value of the test parameter τ_0 becomes $\tau_0=234\pm3$ ps. This value is in good agreement with the lifetime of 231 ± 1 ps obtained in *p*-type GaAs, where no positron trapping at vacancy defects was observed (Sec. IV). In general, the decompositions of the lifetime spectra thus follow well the simple one-trap trapping model at 300 K. However, in a few samples ($n=4.6\times10^{15}$ and 2.5×10^{16} cm^{-3} in Table I) slight discrepancies from the simple trapping model are present. As discussed earlier in Ref. 6, the decomposition at 300 K can be partly influenced by positron trapping at negative ions. However, even when a small contribution from the negative ions is present, the second lifetime τ_2 characterizes positron annihilation at vacancy defects, $\tau_d=\tau_2$ (Sec. III A).

In Table I, the values of τ_2 change in the range 260–290 ps in correlation to the doping level of the sample. Hence, it seems to be that the structure of the vacancy defect changes with carrier concentration of the sample at 300 K. At low doping level, the positron trap can be characterized with roughly $\tau_{d1}=290$ ps, and in highly *n*-type GaAs the positrons get trapped with a lifetime of about $\tau_{d2}=260$ ps, respectively. These values are in good agreement with our earlier results.[2]

B. Temperature effects on the positron lifetimes

In *n*-type GaAs, the average positron lifetime depends strongly on the measurement temperature. The average lifetime as a function of the measurement temperature is shown in Fig. 2 for the various samples studied in this work. The results show the same qualitative behavior as in our earlier works.[2,6,8]

When sample temperature is increased from 10 K, the average positron lifetime increases in all curves of Fig. 2, and it levels off at about 200 K. This increase of τ_{av} with temperature has been discussed in detail elsewhere.[2,6] In *n*-type GaAs positrons localize weakly at Rydberg states of negative ions at low temperatures.[6] The lifetime of positrons trapped at ions is close to the lifetime of 231 ps in bulk GaAs. The decrease of average lifetime below 200 K reflects the competition between trapping processes to vacancies and ions, whereas at high temperature of typically $T>250$ K all positrons are detrapped from ions and only vacancies are seen.[6] In this work, we shall focus

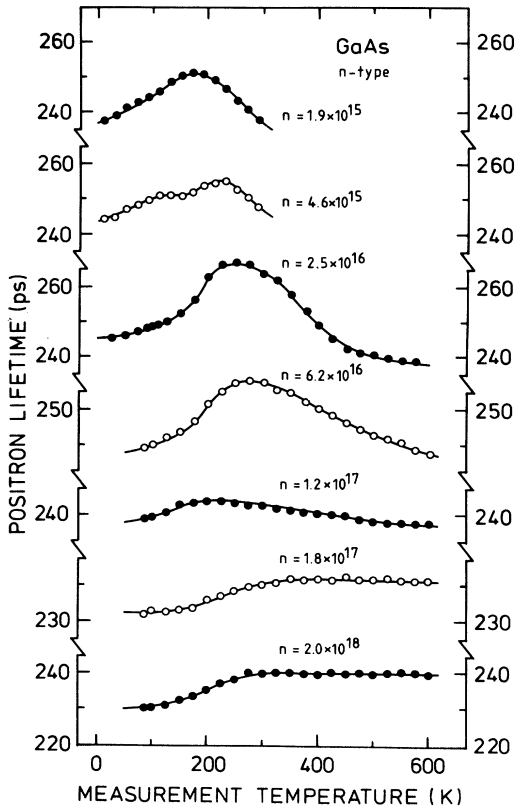

FIG. 2. Positron average lifetime in *n*-type GaAs as a function of measurement temperature. The carrier concentrations in cm^{-3} at 300 K are given in the figure for each sample.

on the properties of the vacancies and we do not concentrate further on temperature effects in τ_{av} below 200 K.

Above 200 K the temperature dependence of τ_{av} is different for the samples with different carrier concentration. In the lightly n-type samples ($n = 10^{15}$–10^{16} cm^{-3}), average lifetime decreases as a function of the measurement temperature. At the intermediate doping level of $n = 10^{17}$ cm^{-3}, this decrease of τ_{av} with temperature becomes much weaker. Finally, in the samples doped to a level of $n = 10^{18}$ cm^{-3} the average positron lifetime is almost independent of temperature at the range $T > 200$ K.

The decomposition of the lifetime spectrum at various measurement temperatures is shown in Fig. 3 for the sample with $n = 2.5 \times 10^{16}$ cm^{-3}. Compared to the room-temperature results (Table I), the decomposition of the lifetime spectrum changes radically when the sample is cooled to low temperatures of 20–100 K. At 20–100 K, the lifetime τ_2 is constant at a value of $\tau_2 = 257 \pm 3$ ps. Between 100 and 250 K, τ_2 increases gradually to the room temperature value of $\tau_2 = 295$ ps, at which it stays constant up to the highest measurement temperature of 575 K. As a function of the sample temperature, the lifetime component τ_2 thus exhibits a transition between two different stable states: 257 ps at low temperature and 295 ps at high temperature.

The strong temperature effects in the average lifetime at $T > 200$ K are also clearly visible in the decompositions of the spectra in Fig. 3. At temperatures above 200 K, the lifetime τ_2 remained constant at 295±3 ps. The large decrease observed in τ_{av} is due to a decrease in the intensity I_2, which drops from 85% to about 40% in the interval 300–600 K. At these temperatures, the increase of τ_1 is consistent with the one-defect trapping model (Sec. III A). On the contrary, at 20–300 K the experimental τ_1 is much larger than expected assuming trapping at one type of vacancy defects only.[6] This behavior is typical, when positions localize at negative ions in addition to vacancies.[6]

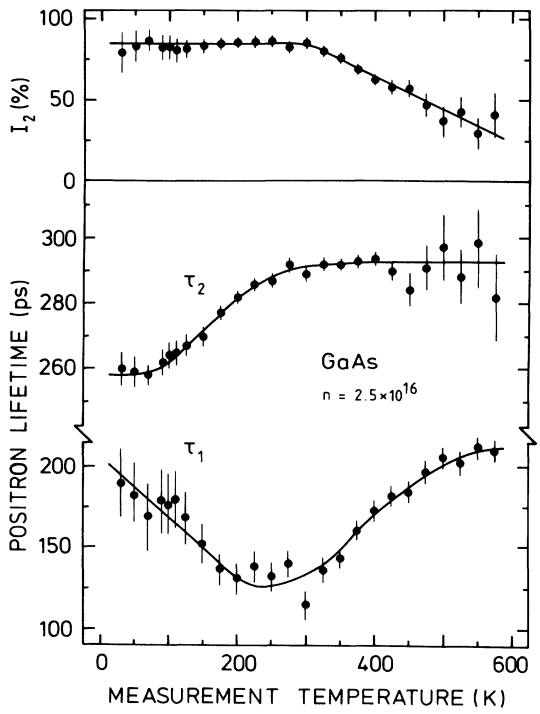

FIG. 3. Decomposition of the positron-lifetime spectrum as a function of temperature in undoped n-type GaAs sample with a carrier concentration of $n = 2.5 \times 10^{16}$ cm^{-3} at room temperature.

Together with the change of the value of τ_2 as a function of temperature, the strong decrease of I_2 at 300–600 K is the most striking result of the decomposition of the lifetime spectra. We shall next discuss successively these two main effects. In particular, we will compare these effects in our various n-type samples, and show that the temperature behavior can be related to the carrier concentration of the sample.

1. Lifetime transition of τ_2 as a function of the sample temperature

The longest lifetime component τ_2 after decomposition of the spectra is shown in Fig. 4 for the various samples studied in this work. For all the measurement temperatures between 10 and 600 K, a free decomposition is not always possible due to a small value of I_2. In these cases, the lifetime component τ_2 is not shown in Fig. 4, although the average lifetime could still be determined (Fig. 2).

In all samples of Fig. 4, the lifetime τ_2 levels off at a value of $\tau_2 = 257 \pm 3$ ps, when the temperature is lowered from 300 K. At 10–50 K, the lifetime of $\tau_2 = 257 \pm 3$ ps is found in all samples, at which the lifetime decomposition was possible. In contrast to room-temperature results (Table I), only one type of positron trap with $\tau_d = 257$ ps is thus found at 10 K independent of the carrier concentration of the sample. The lifetime of $\tau_d = 257$ ps is the same as observed for heavily n-type GaAs at 300 K (Sec. V A and Ref. 2).

When temperature is increased from 10 K, the lifetime component τ_2 increases rapidly from the 257-ps level to about 295 ps in the lightly n-type samples ($n = 10^{15}$–10^{16} cm^{-3}). When the value of $\tau_2 = 295 \pm 3$ ps is reached, τ_2 remains constant as a function of temperature. In the samples with intermediate n-type carrier concentration ($n = 10^{17}$ cm^{-3}), the lifetime τ_2 also increases with temperature, but with a smaller slope compared to the samples with lower n-type doping. Furthermore, no saturation of τ_2 could be observed at high temperatures in the samples with $n = 10^{17}$ cm^{-3}, and the onset of the increase in τ_2 is shifted to higher temperatures than in the samples with $n = 10^{15}$-cm^{-3} doping range. Finally, in heavily n-type GaAs the lifetime τ_2 remains at 260±3 ps at all measurement temperatures up to 600 K.

Changes in the lifetime τ_2 with temperature are observed in Fig. 4 for various n-type GaAs samples with the donor concentration ranging from 10^{15}–10^{17} cm^{-3}. As a function of temperature, τ_2 shows also saturations at 257±3 ps at 10–100 K and at 295±3 ps at high temperatures. This suggests that the values $\tau_2 = 257 \pm 3$ and

295±3 ps are two well-defined levels of the positron lifetime τ_2, and the temperature dependence of τ_2 in Fig. 4 reflects an equilibrium between these two possible annihilation states. Hence, the lifetime transition $\tau_2=257\rightarrow295$ ps at 10–600 K seems to be a general property of the positron lifetime τ_2 at the 10^{15}–10^{17}-cm^{-3} doping range.

The transition $\tau_2=257\rightarrow295$ ps in Fig. 4 shows also systematic trends, which correlate to the carrier concentration of the sample. The arrow in each of the τ_2 curves in Fig. 4 indicates the center temperature, at which the lifetime τ_2 is in the middle of the transition at $\tau_2=276$ ps. In the sample with the lowest n-type conductivity ($n=1.9\times10^{15}$ cm^{-3}), the middle of the transition is located at 80 K. When the carrier concentration increases, the value of $\tau_2=276$ ps is obtained systematically at higher temperatures, and in the sample with $n=1.8\times10^{17}$ cm^{-3} a temperature of 550 K is required to reach the middle of the lifetime transition $\tau_2=257\rightarrow295$ ps. Finally, in heavily n-type GaAs ($n=2\times10^{18}$ cm^{-3}) the changes in τ_2 are not present in the measurement temperature range of 10–600 K. Hence, in the samples with higher carrier concentration, the lifetime transition $\tau_2=257\rightarrow295$ ps is shifted systematically to higher temperatures.

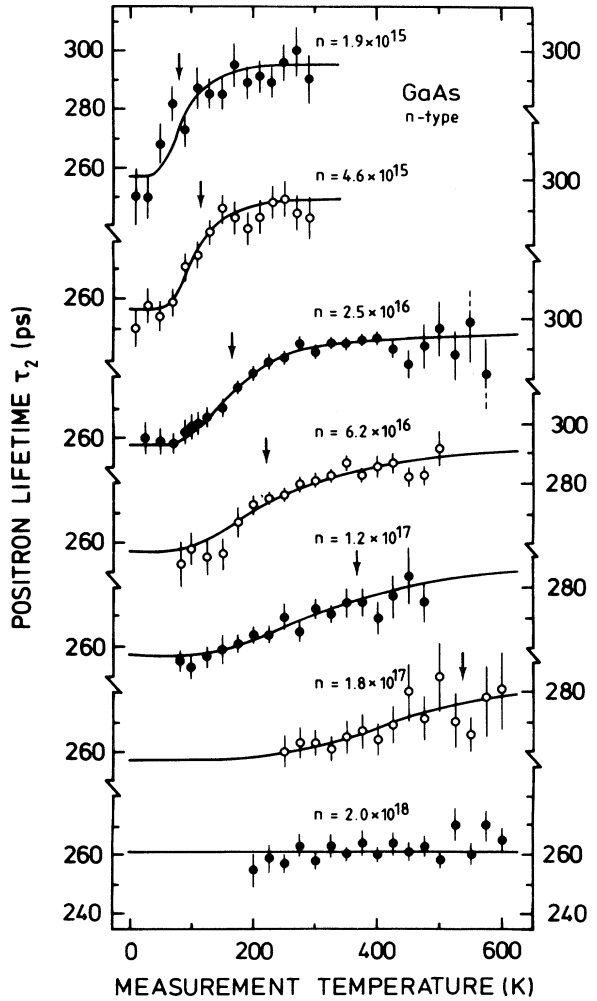

FIG. 4. Positron lifetime τ_2 at vacancy defect as a function of measurement temperature. The arrows indicate the middle of the lifetime transition from $\tau_2=257$ to 295 ps. The solid lines are fits of Eq. (21) with the value of ionization level E_i given in Table II for each of the curves. The carrier concentrations n are given in cm^{-3} in the figure.

In addition to the middle temperature, the temperature width of the lifetime transition $\tau_2=257\rightarrow295$ ps changes radically in the samples with different carrier concentrations. In the sample with $n=1.9\times10^{15}$ cm^{-3} the total range of changes in τ_2 is only 100 K, whereas at least a temperature interval of 600 K is required for the complete transition in the samples with 10^{17} cm^{-3} conduction electrons. For all curves in Fig. 4, the width of the changes in the lifetime τ_2 is thus systematically correlated to the carrier concentration of the sample, or possibly to the temperature, at which the transition $\tau_2=257\rightarrow295$ ps takes place.

We summarize the temperature effects on the decomposed lifetime τ_2 as follows. (i) As a function of temperature, the lifetime τ_2 changes between two well-defined levels of 257±3 ps and 295±3 ps. (ii) The transition $\tau_2=257$ ps$\rightarrow$295 ps is shifted to higher temperatures, when the carrier concentration of the sample decreases. (iii) The temperature width of the transition $\tau_2=257\rightarrow295$ ps increases, when the transition occurs at higher temperature.

2. *Decrease of positron trapping as a function of the sample temperature*

In Fig. 2, the average positron lifetime was seen to decrease in the lightly n-type samples ($n=10^{15}$–10^{16} cm^{-3}) as a function of temperature at 200–600 K. During this decrease, the lifetime of the trapped positron τ_2 stays constant at $\tau_2=295$ ps, and the decomposition follows well the simple trapping model with only one type of vacancy defects. The changes in τ_{av} can thus be characterized with the positron trapping rate κ calculated from the one-defect trapping model [Eq. (7)].

Figure 5 shows the positron-trapping rate as a function of temperature in various lightly n-type samples studied in this work. The decrease in τ_{av} seen in Fig. 2 corresponds to the decrease of κ in Fig. 5. The largest values of κ in the various samples in Fig. 5 range between 2–7 ns^{-1}, and the absolute levels of the trapping rates do not seem to be correlated to the carrier concentrations of the samples.

The arrow in Fig. 5 indicates the temperature, at which the trapping rate κ has decreased to half of the value obtained at low temperatures before the changes in κ take place. In the sample with the lowest carrier concentration of $n=1.9\times10^{15}$ cm^{-3}, the trapping rate starts to decrease at about 200 K, and it drops to half of the original value already at 260 K. A further increase of the measurement temperature results in a decrease in κ, and no saturation of the trapping rate is obtained at 300 K. In the sample with an order-of-magnitude larger carrier concentration ($n=2.5\times10^{16}$ cm^{-3}), the decrease of κ

starts at about 260 K, and a temperature of 370 K is required to decrease the trapping rate to the half of its value at 250 K. In the sample with further increased doping ($n=6.2\times10^{16}$ cm^{-3}), both the onset and the middle of the $\kappa=\kappa(T)$ curve are still shifted to higher temperatures, to about 280 and 410 K, respectively. At the same time the temperature width of the change in the trapping rate becomes much larger. In the sample with $n=6.2\times10^{16}$ cm^{-3}, κ decreases over a temperature interval of 400 K, whereas in the $n=1.9\times10^{15}$ cm^{-3} sample only about 150 K is needed to decrease the trapping rate to about 0 ns^{-1} from its original level.

The middle temperature (arrow in Fig. 5) is thus shifted from 260 to 410 K, when the carrier concentration is increased roughly 30 times from 1.9×10^{15} to 6.2×10^{16} cm^{-3}. At the same time, the shape of the $\kappa=\kappa(T)$ curve becomes much wider. Hence, the decrease of trapping rate as a function of temperature seems to be correlated to the carrier concentration of the sample. When compared to the temperature behavior of the decomposition of the lifetime spectra (Sec. V B 1), the trapping rate κ exhibits similar properties as the lifetime component τ_2. As functions of temperature, both parameters show transitions, which can be related to the carrier concentration of the samples.

We summarize as follows our experimental findings of the temperature dependence of the lifetime spectra in n-type GaAs. We have observed two positron-lifetime transitions, which correlate to the carrier concentration of the sample. In the first transition, the lifetime of the trapped positron changes from 257±3 to 295±3 ps. In the second transition, the positron trapping rate decreases towards zero.

VI. DISCUSSION

In this section, we shall attribute the positron traps in n-type GaAs to monovacancies in As sublattice. Furthermore, we shall discuss the temperature effects in the positron lifetimes in terms of the ionization processes of V_{As}, and determine the corresponding positions of the ionization levels in the energy gap. Finally, we shall conclude that large lattice relaxations are associated with the ionization of V_{As}. We suggest that the negative configuration of V_{As} is about 10% inward relaxed compared to the neutral V_{As}.

A. Properties of positron traps in the n-type GaAs

In n-type GaAs, positron trapping at vacancy-type defects is always observed. The two-component analyses in Table I indicate that positrons are trapped with a second lifetime τ_2 of the range of 257–295 ps. The lifetimes τ_2 measured in various samples at 300 K are collected in Fig. 6 as a function of the carrier concentration at 300 K. We have also included in Fig. 6 data from our earlier measurements.[2,6,16]

In Fig. 6, the lifetime of the trapped positron τ_2 is constant $\tau_2=295\pm3$ ps in all samples with a low carrier concentration between 1.9×10^{15} and 2.5×10^{16} cm^{-3}. Similarly, when the carrier concentration is high in the level

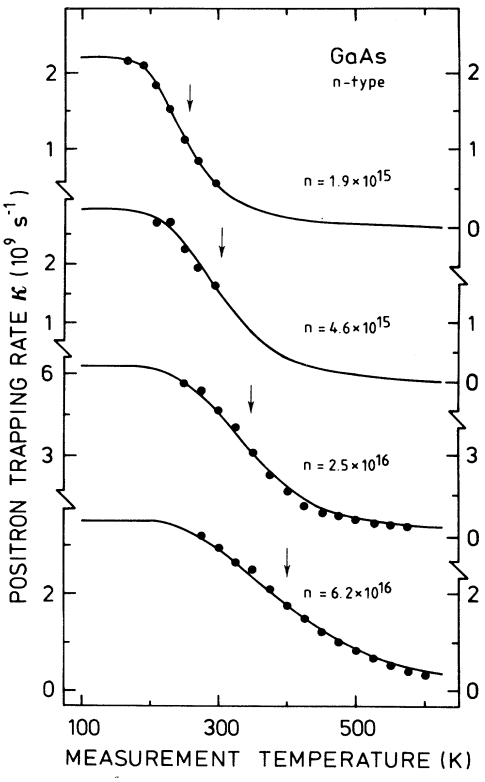

FIG. 5. Positron trapping rate κ at vacancy defect as a function of measurement temperature. The solid lines are fits of the Fermi function [Eq. (24)] with degeneracy factor $g=4$ and with the value of the ionization level E_i given in Table III for each of the curves. The arrows indicate the middle of the transition $\kappa\rightarrow0$. The carrier concentrations n are given in cm^{-3} in the figure.

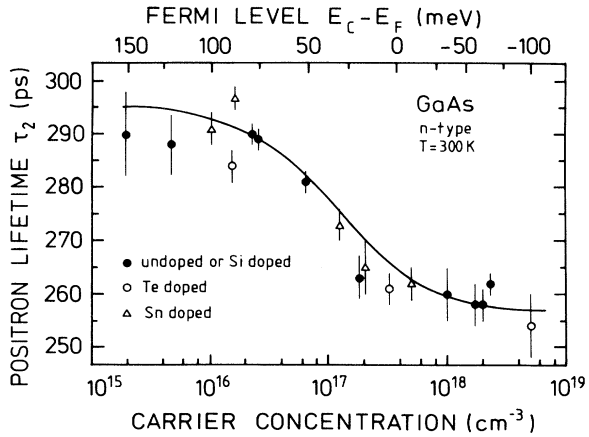

FIG. 6. Positron lifetime τ_2 at vacancy defect in samples studied in this work or in our previous works (Refs. 2, 6, and 16). The calculated position of the Fermi level E_F is given in reference to the bottom of the conduction band E_C. The solid line is a fit of Eq. (21) with an ionization level of vacancy defect at $E_C-E_i=30$ meV. All measurements have been performed at constant temperature of 300 K.

of 5×10^{17} to 5×10^{18} cm^{-3}, the second lifetime is again independent of doping and gets a value of $\tau_2=257\pm3$ ps. In the intermediate carrier-concentration range of 3×10^{16} to 5×10^{17} cm^{-3}, τ_2 decreases continuously from the 295-ps level towards the value of 257 ps obtained in the highly doped material. The room-temperature data of Fig. 6 thus suggests that the lifetimes $\tau_2=257\pm3$ and 295 ± 3 ps correspond to two well-defined annihilation states at the vacancy defects, whereas the lifetimes $\tau_2=260-290$ ps obtained in the $n=10^{17}$-cm^{-3} doping range are rather superpositions of the levels of 257 and 295 ps.

The same trend can be seen also in the data measured as a function of temperature. At low temperatures, only one type of positron trap with a lifetime of 257 ± 3 ps is present in all samples (Fig. 4). When temperature is increased, τ_2 increases and finally saturates at the lifetime value of 295 ± 3 ps. Hence, two levels of τ_2 are found also in temperature dependence of τ_2: The lifetime of the trapped positron saturates at either $\tau_2=257\pm3$ or 295 ± 3 ps, when the temperature of the sample is changed. We can thus conclude that two different vacancy defects act as positron traps in n-type GaAs, and they correspond to the positron lifetimes of $\tau_2=257\pm3$ and 295 ± 3 ps, respectively.

The lifetime of $\tau_2=295$ ps is 28% higher than the bulk lifetime of $\tau_b=231$ ps in GaAs. This value is close to the lifetime ratio (273 ps)/(220 ps)=1.24 that we have previously found for a negative monovacancy in electron irradiated Si.[10] In electron-irradiated Ge, we have observed positron trapping at monovacancies with a lifetime of 290 ps, which is 26% higher than the bulk lifetime of $\tau_b=230$ in Ge.[17] The comparison to the observed lifetimes in monovacancies in Si in Ge thus suggests that the lifetime of 295 ps in GaAs is due to positron trapping and annihilation at monovacancy defects.

This interpretation is supported also by the theoretical calculations of positron lifetimes. The calculations with self-consistent electron structure predict values of 279 and 267 ps for neutral unrelaxed V_{As} and V_{Ga}, respectively.[18] For unrelaxed divacancies $V_{Ga}V_{As}$, the calculated positron lifetime is about 320 ps.[19] This lifetime is much longer than found in any of our n-type samples. We can thus conclude that both the experiments in Si and Ge as well as the theoretical calculations are in agreement that the trapped-positron lifetime of 295 ps corresponds to positron annihilation at a monovacancy defect.

The positron lifetime of $\tau_2=257\pm3$ ps is smaller than the value of $\tau_2=295$ ps, indicating a smaller open volume. The value of $\tau_2=257$ ps is in good agreement with the results in electron-irradiated GaAs, where positron trapping to Ga monovacancies has been observed with a lifetime of 260 ± 5 ps.[8,20,21] The ratio (257 ps)/(231 ps)=1.11 is also in good agreement with the measurements in electron-irradiated P-doped Si, where the negative vacancy-phosphorus pair (V-P) has been found to trap positrons with a ratio (248 ps)/(220 ps)=1.13.[10,22] The theoretical estimates of 260–280 ps for positron lifetimes in monovacancies in GaAs give further support to attribute also the positron trap with $\tau_2=257$ ps to a monovacancy.[18,19] Based on all these arguments, we conclude that also the position trap with $\tau_2=257$ ps is due to annihilations at a monovacancy defect.

To summarize, two different positron traps with lifetimes 257 and 295 ps are observed in n-type GaAs. The 257-ps configuration is present at low temperatures and in highly doped samples, whereas the 295-ps configuration exists at high temperatures and in the samples with low carrier concentration. In the intermediate temperature and doping ranges, the two positron traps coexist and the resulting lifetime takes any value between 257 and 295 ps. Both positron traps correspond to annihilations at monovacancy defects.

B. Lifetime transition 257→295 ps and the ionization of a vacancy defect

1. Positron lifetimes at vacancies and the position of the Fermi level

The results in Fig. 6 show that the monovacancy with 295-ps positron lifetime is gradually replaced by the configuration with $\tau_2=257$ ps, when the carrier concentration at 300 K increases. This transition 257 ps↔295 ps occurs also as a function of temperature. In Fig. 4, the monovacancy with the 257-ps lifetime becomes less dominant when temperature increases, and finally it is completely replaced by the monovacancy with $\tau_2=295$ ps. The transition temperature becomes higher when the carrier concentration increases. This suggests that the transition 257 ps↔295 ps is not a pure temperature effect, but it is rather related to the free-electron density of the sample. This interpretation is further supported by the data in Fig. 6, where the transition 257 ps↔295 ps occurs as a function of carrier concentration at *constant* temperature of 300 K.

The lifetime of the trapped positron seems thus to be related to both the initial doping level and the crystal temperature. In thermal equilibrium, the effects of these two quantities can be described by a single parameter, the Fermi level E_F. When temperature is decreased in n-type semiconductor, the electron levels in the energy gap become more populated, and the Fermi level moves towards the conduction band. The same shift of the Fermi level can be obtained also by increasing the donor concentration at constant temperature.

Hence the ionization of the defect levels in the gap is determined by the Fermi level.[13] When the Fermi level is close to the conduction band, a defect is in its most negative state. When temperature is increased, the Fermi level moves toward the midgap, and the defect can change its charge, if the Fermi level crosses an ionization level of the defect. Because the Fermi level depends on the doping concentration in addition to temperature, the ionization of the defect takes place at higher temperatures in the samples with a larger carrier concentration at 300 K. This suggests that the positron-lifetime transition 257 ps↔295 ps between two monovacancy defects is a Fermi-level controlled process.

Figure 7 shows the positron lifetime τ_2 in the vacancy

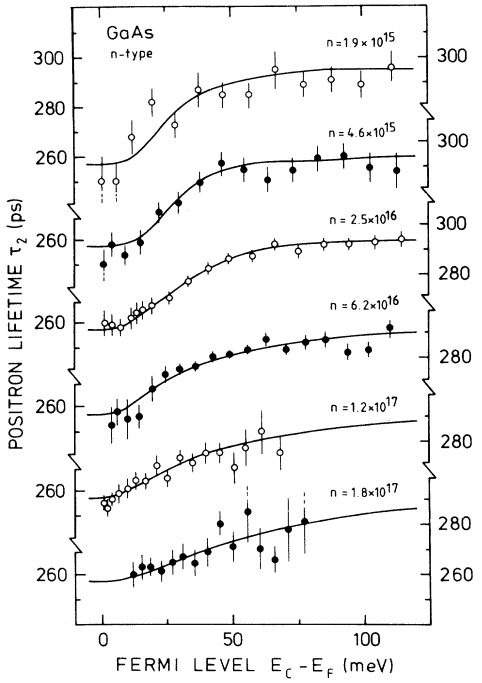

FIG. 7. Positron lifetime τ_2 at vacancy defect as a function of the position of the Fermi level E_F in reference to the bottom of the conduction band E_C. The solid line is a fit of Eq. (21) with an ionization level of vacancy defect E_i given in Table II for each of the curves. The carrier concentrations n are given in cm^{-3} in the figure.

as a function of the Fermi-level position in the energy gap. The Fermi level E_F at temperature T was calculated from the carrier concentration n as $n = N_c F_{1/2}(E_F, T)$, where N_c is the effective density of states of the conduction band and $F_{1/2}$ the Fermi integral.[23] The temperature dependence of E_F was calculated assuming that the conduction electrons are emitted from a single shallow donor at 3–6 meV below the conduction band.[24] This assumption was checked by Hall experiments in several samples at 300 and 77 K, and a good agreement with our calculations was found for the temperature dependence of E_F.

In Fig. 7, the lifetime τ_2 gets a value of $\tau_2 = 257 \pm 3$ ps in all samples at the Fermi-level positron close to the conduction band at $E_C - E_F = 0$–15 meV. When the Fermi level moves toward the midgap, the positron lifetime τ_2 starts to increase in all samples. This increase continues roughly over the interval $E_C - E_F = 15$–50 meV, after which τ_2 saturates at a value of 295 ps. Figure 7 shows thus clearly that the 257 ps $\leftrightarrow$295 ps transition in τ_2 takes place in all samples at the same position of the Fermi level, although the measurements in Fig. 7 have been performed at different temperatures of $T = 10$–600 K and in many samples with carrier concentrations ranging two orders of magnitude from $n = 1.9 \times 10^{15}$ to $n = 1.8 \times 10^{17}$ cm^{-3} at 300 K.

The calculated position of the Fermi level is indicated also in Fig. 6, which shows the positron lifetime τ_2 as a function of carrier concentration at constant temperature of 300 K. When the carrier concentration of the sample decreases, the Fermi level moves towards midgap. At the same time, the lifetime of the trapped positron changes from $\tau_2 = 257$ ps to $\tau_2 = 295$ ps. In Fig. 6, the lifetime τ_2 thus exhibits a transition 257 ps$\leftrightarrow$295 ps, when the position of the Fermi level is changed by varying the carrier concentration of the sample at constant temperature of 300 K. This behavior is in perfect agreement with the data in Fig. 7, where the position of the Fermi level was moved by changing the measurement temperature. The transition of positron lifetime τ_2 between the two values 257 and 295 ps is thus controlled by the position of the Fermi level in the energy gap.

The defects with positron lifetimes of 257 and 295 ps were attributed to monovacancies in the previous section. The transition 257ps$\leftrightarrow$295 ps thus shows that a monovacancy ($\tau_2 = 257$ ps) is replaced by a second type of a monovacancy ($\tau_2 = 295$ ps), when the Fermi level reaches a well-defined position in the energy gap. The simplest of such processes is the ionization of the monovacancy. When the positron lifetimes in two different charge states of the vacancy differ sufficiently, the ionization process is observed as a transition in the trapped-positron lifetime, when the Fermi level moves in the energy gap (Sec. III). Our results in n-type GaAs follow exactly this kind of behavior: a monovacancy with $\tau_2 = 257$ ps is replaced by a second monovacancy with $\tau_2 = 295$ ps as a function of the Fermi-level position. We can thus conclude that the two types of monovacancies observed are not independent defects, but their concentrations are related through the Fermi distribution. We attribute them to two different charge states of the same monovacancy defect.

2. *Determination of the ionization level*

The ionization process of the monovacancy can be quantitatively analyzed in terms of the trapping models introduced in Sec. III. When the positron lifetime is different in the two charge states of the vacancy, we can use Eq. (21) to model the experimental data with $\tau_A = 257$ ps and $\tau_B = 295$ ps as lifetime values at the charge states A and B, respectively. We emphasize that strictly speaking Eq. (21) is valid only if the positron-trapping rates at vacancies are high enough compared to annihilation rates at vacancies and in the bulk (see Sec. III B 1). However, a quantitative analysis shows that with our values of τ_A, τ_B, and τ_b, Eq. (21) is still a good approximation even when the trapping rates κ_A and κ_B get such small values as 0.2 ns^{-1}. For example, when κ_A and κ_B vary in the range 0.2–20 ns^{-1}, the simplifying approximations affect the values of τ_2 in Eq. (21) by less than 2 ps only. This value is clearly smaller than typical statistical errors in the experimental lifetime components. Hence, the quantitative analysis of our data is possible with the trapping models of Sec. III.

The best fits of Eq. (21) to the experimental τ_2 are indicated by solid lines in Figs. 4 and 7. In these fits, we have simply omitted the influence of the degeneracy factor g and the positron trapping coefficients μ_{eff} ($g = 1$, $\mu_{\text{eff}} = 1$). The fitted values of the ionization level E_i are given for

each of the samples in Table II.

The solid lines in Figs. 4 and 7 reproduce well the experimentally observed behavior of τ_2. The shape of the Fermi function f_{e+} fits well to τ_2, and the width of the transition 257 ps↔295 ps is seen to increase considerably, when the transition is shifted to higher temperatures. The good quantitative agreement between the experiments and the shape of the Fermi functions in Eq. (21) thus provides further support that the observed behavior of τ_2 can be assigned to an ionization process of a monovacancy.

The fitted values of the ionization level $E_C - E_i$ are given in Table II. In the lightly to intermediate doped samples with $n = 1.9\times10^{15}$ to 6.2×10^{16} cm^{-3}, the ionization level is found exactly at the same position in the energy gap at $E_C - E_i = 30\pm3$ meV. The degeneracy factors g and the trapping coefficients μ_{eff} being omitted in the fitting, the ionization level $E_C - E_i = 30\pm3$ meV in Fig. 7 is located in the middle ($f_{e+} = 0.5$) of the transition 257 ps↔295 ps. In the two samples with the carrier concentration in the $n = 10^{17}$-cm^{-3} range, the fitted ionization level gets slightly larger values of $E_C - E_i = 45, \ldots, 65$ meV. As will be discussed later, we feel that these larger values are rather due to difficulties in the exact determination of the Fermi level than "real" changes in the position of the ionization level of the vacancy defect.

In addition to the temperature behavior of τ_2, the ionization level $E_C - E_i$ can also be obtained from the room-temperature data of Fig. 6. At 300 K, the Fermi level can be directly calculated from the measured carrier concentration, and no assumptions of the temperature dependence have to be done. The values of $E_C - E_F$ are indicated for all samples in Fig. 6, and the solid line corresponds to a fit of Eq. (21) with a vacancy ionization level at $E_C - 30$ meV. In Fig. 6 it is evident that the room-temperature data is in a good agreement with the temperature behavior of τ_2. The same Fermi functions f_{e+} with an ionization level at $E_C - 30$ meV can be used to model both types of data. The dependence of τ_2 on both temperature and carrier concentrations can thus be explained with a single parameter, the Fermi level E_F.

In a more detailed analysis of the ionization level, we have to take into account the effects of the degeneracy factor g and the dependence of positron trapping coefficient on the charge of the vacancy. Unfortunately, the internal degeneracies of the monovacancies in GaAs are not well known. In addition to spin degeneracy, the possible lattice relaxations at the ionization process can also have large influence on the value of g, and, consequently, on the Fermi function f_{e+}. However, the *experimental* determination of g from the shape of the $\tau_2 = \tau_2(E_F)$ curve is unreliable due to statistical scattering in the lifetime component τ_2.

In principle, the ratio of the positron trapping coefficients μ_{eff} could be determined from the trapping rates κ at the two monovacancy defects on both sides of the transition 257 ps↔295 ps. However, at low temperatures of $T < 150$ K this is not possible due to additional positron trapping at negative ions.[6] The trapping coefficients μ_A and μ_B can also have different temperature dependencies, which result in a temperature dependent ratio μ_{eff}. In our results, experimental information of μ_{eff} can only be obtained from the sample with $n = 1.2\times10^{17}$ cm^{-3}. In this sample, the transition 257↔295 ps occurs at a temperature range of 200–600 K, where the negative ions do not have an influence on the average lifetime.

In the sample with $n = 1.2\times10^{17}$ cm^{-3}, the average positron lifetime decreases with temperature from 243 ps at 200 K to about 238.5 ps at 600 K. The decrease of τ_{av} takes place during the transition 257 ps↔295 ps, i.e., during an increase in the second lifetime τ_2. This is a clear sign that the positron trapping coefficient is smaller in the monovacancy with $\tau_d = 295$ ps than in the configuration with $\tau_d = 257$ ps. Using Eq. (7), the positron trapping rates at the two monovacancies become $\kappa_A = 3.7$ ns^{-1} ($\tau_d = 257$ ps, $T = 150$ K) and $\kappa_B = 0.58$ ns^{-1} ($\tau_d = 295$ ps, $T = 600$ K). The ratio of the trapping coefficients at the two monovacancy defects is thus $\mu_{\text{eff}} = \mu_A/\mu_B = \kappa_A/\kappa_B = 6\pm1$. However, we have to emphasize that this value is only a rough estimate, because we have omitted the possible temperature dependence of the positron-trapping coefficients.

The influence of g and μ_{eff} on the ionization level $E_C - E_i$ of the monovacancy was tested by fitting Eq. (21) to the experimental data with the ratio $\mu_{\text{eff}}/g = 2.5$. With a value of $\mu_{\text{eff}} = 5$, the ratio $\mu_{\text{eff}}/g = 2.5$ thus corresponds to a degeneracy factor of $g = Z_B/Z_A = 2$. This spin degeneracy can be expected if the vacancy changes,

TABLE II. The fitted ionization levels in various samples in the lifetime transition 257↔295 ps of the native monovacancy defect. The influence of the positron-trapping coefficients is studied by changing the parameter μ_{eff}, which is the ratio of the trapping coefficients at monovacancies with positron lifetimes of 257 and 295 ps, respectively. g is the degeneracy factor of the ionization level.

Carrier concentration (cm^{-3})	Ionization level (meV) with $g = 1$ and $\mu_{\text{eff}} = 1$	Ionization level (meV) with $\mu_{\text{eff}}/g = 2.5$
1.9×10^{15}	27±5	20±4
4.6×10^{15}	30±5	22±4
2.5×10^{16}	30±4	20±3
6.2×10^{16}	32±6	17±4
1.2×10^{17}	45±9	22±5
1.8×10^{17}	65±15	35±9

e.g., from a spin-paired configuration ($Z_A=1$) to a charge state with one unpaired electron ($Z_B=2$). Using these parameters to fit Eq. (21) to the experimental data (Figs. 4 and 7), the ionization level E_C-E_i gets the values also given for all samples in Table II.

The experimental lifetime component τ_2 could well be modeled with Fermi functions f_{e+} with $\mu_{\rm eff}/g=2.5$, and the best fits do not differ noticeably from the solid lines in Figs. 4 and 7. In all samples with the carrier concentration of $n=1.9\times10^{15}$ to 1.2×10^{17} cm^{-3}, the same values of $E_C-E_i=20\pm3$ meV were obtained for the ionization level E_C-E_i. Also in the analysis of the room-temperature data of Fig. 6 with $\mu_{\rm eff}/g=2.5$, the position of the ionization level was obtained as $E_C-E_i=20\pm5$ meV. This value is smaller than the result $E_C-E_i=30\pm3$ meV found in the previous analysis, where the trapping coefficients of the degeneracy factors were omitted ($\mu_{\rm eff}=1$ and $g=1$). In conclusion, the influence of these parameters to the position of the monovacancy ionization level at E_C-30 meV is thus typically 10 meV.

In the sample with $n=1.8\times10^{17}$ cm^{-3}, a slightly higher value of $E_C-E_i=35$ meV was obtained for the ionization level E_C-E_i of the monovacancy defect. The same tendency was found also in the fits with $\mu_{\rm eff}=1$ and $g=1$. However, we feel that this discrepancy is mostly due to the difficulties in the exact determination of the Fermi level, because we have omitted the following complications in our simple calculation of E_F: (i) the effective mass of the conduction electrons depends on temperature at 20–600 K,[23] (ii) the conduction band is not completely parabolic, which changes the effective density of states especially, when $n>10^{17}$ cm^{-3},[23] and (iii) the donor atoms are not independent of each other at the doping level of 10^{17} cm^{-3},[25] and the formation of the consequent impurity band changes the temperature dependence of the Fermi level. Due to these difficulties in the analysis of the samples with a carrier concentration of the order of 10^{17} cm^{-3}, we feel that the values of E_C-E_i obtained in the lightly n-type samples ($n=10^{15}$–10^{16} cm^{-3}) are more reliable.

We can thus summarize our analysis of the temperature dependence of τ_2 as follows. We have found a reversible transition between two different types of monovacancies, and we attribute it to an ionization process. The transition is controlled by the position of the Fermi level in the energy gap, and it takes place when the Fermi level crosses an ionization level at $E_C-E_i=30\pm3$ meV. This value is affected typically 10 meV by different values of the degeneracy factors and the positron trapping coefficients at the two charge states of the monovacancy involved.

C. Transition in the positron-trapping rate $\kappa\rightarrow0$

After the lifetime transition 257 ps↔295 ps in the trapped-positron lifetime τ_2, the average lifetime is observed to decrease strongly as a function of temperature (Fig. 2). During this decrease, the lifetime component τ_2 remains constant ($\tau_2=295$ ps). The decrease in $\tau_{\rm av}$ is shown in Fig. 5 in terms of the positron-trapping rate κ, which is calculated from the one-defect trapping model using Eq. (7). It is especially interesting to note that the changes in κ are shifted to higher temperatures when the carrier concentration of the sample increases. This suggests strongly that the transition $\kappa\rightarrow0$ is controlled by the Fermi level in a similar way as discussed above in the case of τ_2.

The positron-trapping rate is shown in Fig. 8 as a function of the Fermi-level position in the energy gap. The trapping rate κ has been normalized to the value κ_0 obtained at low temperatures before the transition takes place (Table III). In Fig. 8 it can be directly seen that the decrease of the trapping rate from the κ_0 level occurs in all samples at the same position of the Fermi level, although the carrier concentrations and the measurement temperatures are different for each of the curves. Hence, the transition $\kappa\rightarrow0$ seems to be a Fermi-level controlled process.

The simplest Fermi-level controlled process with a decrease in the positron trapping rate is an ionization of a vacancy defect with a subsequent decrease in the trapping coefficient μ. The vacancy with $\tau_2=295$ ps was attributed in Sec. VI A to a monovacancy. The change observed as a function of the Fermi level corresponds thus to an ionization at which the monovacancy changes to a more positive charge state by emitting an electron. In good

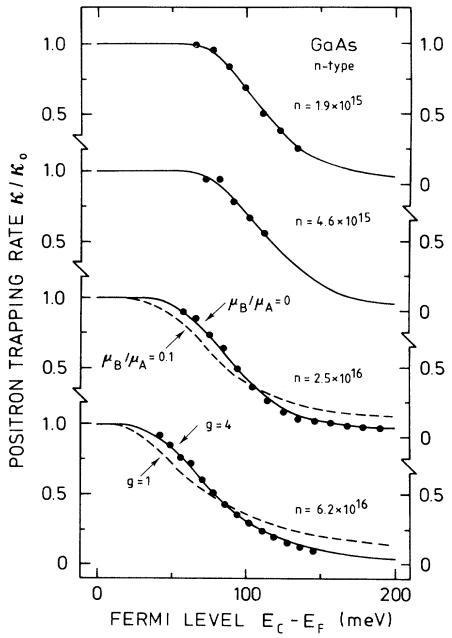

FIG. 8. Positron-trapping rate κ at vacancy defect as a function of the position of the Fermi level E_F in reference to the bottom of the conduction band E_C. The solid lines are fits of Eq. (24) with an ionization level of vacancy defect E_i given in Table III for each of the curves. The influences of the positron-trapping coefficients μ_B/μ_A and degeneracy factors g to the fits are demonstrated for two of the samples. The carrier concentration n are given in cm^{-3} in the figure.

TABLE III. The fitted ionization levels in various samples in the transition of the positron-trapping rate $\kappa \rightarrow 0$ of the native monovacancy defect. The influence of the degeneracy factor g is studied with fits corresponding to $g=1$ and $g=4$, respectively. κ_0 is the estimated value of positron-trapping rate before the transition $\kappa \rightarrow 0$ occurs.

Carrier concentration (cm^{-3})	Trapping rate κ_0 (ns^{-1})	Ionization level (meV) with $g=1$	Ionization level (meV) with $g=4$
1.9×10^{15}	2.2	115±11	145±14
4.6×10^{15}	2.9	120±12	155±16
2.5×10^{16}	6.3	90±7	133±10
6.2×10^{16}	3.5	75±6	125±10

qualitative agreement with theory,[11] the trapping coefficient and thus the trapping rate decreases in Fig. 8, when the vacancy defect becomes more positive.

The ionization level of the transition $\kappa \rightarrow 0$ can be obtained by fitting Eq. (24) to the experimental trapping rate κ. In Eq. (24), the ratio of the positron-trapping coefficients μ_B/μ_A and the degeneracy factor g are unknown parameters in addition to the ionization level E_i. First, we have fixed g at different values between 0.5 and 6 and studied the effects of the ratio μ_B/μ_A. This quantitative analysis is illustrated in Fig. 8 with the crystal doped at the carrier concentration of $n=2.5\times10^{16}$ cm^{-3}.

In the sample with $n=2.5\times10^{16}$ cm^{-3}, the analysis shows that ratios less than $\mu_B/\mu_A=0.03$ must be applied in order to fit Eq. (24) to the experimental data, when g varies in the range of $g=0.5-6$. These values of μ_B/μ_A are much smaller than the ones which can be deduced from the trapping rates at 250 and 550 K. The trapping rates at 250 and 550 K are 5.6 and 0.42 ns^{-1}, which suggests that the ratio of the trapping coefficients would be roughly $\mu_B/\mu_A \approx 0.1$. However, the fit of Eq. (24) with $\mu_B/\mu_A=0.1$ yields to much too high values of κ at large E_C-E_F (Fig. 8), thus indicating that the ratio $\mu_B/\mu_A=0.1$ is much too large to reproduce the experimental data by Eq. (24). Therefore, the trapping coefficient must decrease by more than a factor of 10 in the transition of the trapping rate in Fig. 8. In practice, we can thus conclude that the trapping coefficient is changed to zero in the transition of Fig. 8, and the exponential tail of the Fermi function is able to explain the slow decrease of the trapping rate at 400–600 K in Figs. 5 and 8.

When the second term in Eq. (24) is omitted due to $\mu_B/\mu_A \rightarrow 0$, the transition $\kappa \rightarrow 0$ can be described directly by the Fermi function of the ionization of a monovacancy. In addition to the ionization level E_i, the shape of the Fermi function f is also determined by the degeneracy factor $g=Z_B/Z_A$ [Eq. (11)]. To study the influence of g we have varied it at the range of $g=0.5-6$ with μ_B/μ_A fixed to zero as explained above. Fits with $g=1$ and $g=4$ are shown in Fig. 8 for the data measured in the sample with $n=6.2\times10^{16}$ cm^{-3}. As seen in Fig. 8, the nondegenerate Fermi functions ($g=1$) are much too broad to fit to the experimental values of positron-trapping rate. A value of $g=4$ was required to reproduce well the shape of the experimental κ in all four curves of Fig. 8. This suggests that a relatively large change in the internal degeneracy is present in the ionization process of the monovacancy. Furthermore, the degeneracy Z_B of the charge state with no positron trapping seems to be clearly larger than the degeneracy Z_A of the state corresponding to positron trapping with $\tau_2=295$ ps.

The fitted values of the ionization level E_i of the transition $\kappa \rightarrow 0$ are given for the degeneracies $g=1$ and $g=4$ in Table III. The solid lines in Figs. 5 and 8 correspond to fits with $g=4$. With this degeneracy, the ionization level gets values in the range of 125–155 meV in all samples. As a mean value of the data, the ionization level of the monovacancy is thus found at 140±15 meV below the conduction band. The fits with no degeneracy factor ($g=1$) yield a lower value of $E_C-E_i=100\pm15$ meV. The ionization level is thus at 100–140 meV at any reasonable value of the degeneracy factor g.

In conclusion, we have observed a Fermi-level-controlled transition in the positron-lifetime spectrum, at which the trapping coefficient to a monovacancy defect decreases to zero. We attribute it to an ionization process of the monovacancy to a less negative state. The ionization level is at 140±15 meV below the conduction band. This value is affected less than 40 meV by the different degeneracies of the ionization level.

D. Identification of the ionization processes

To summarize the analysis explained in the previous sections, we have observed two ionization processes of a monovacancy defect, when the Fermi level moves in the upper part of the energy gap. The ionization takes place at $E_C-E_i=30$ meV and at $E_C-E_i=140$ meV. In the first process, the positron lifetime in the vacancy defect changes radically from 257 to 295 ps. The second ionization can be characterized by a large decrease in the positron-trapping coefficient. In this section we shall discuss the origin of these transitions and attribute them to the ionization of the As vacancy.

The monovacancies in GaAs can exist in either the Ga or the As sublattice. From theoretical calculations,[26–28] it has been generally accepted that the ionization levels of V_{Ga} are in the lower half of the energy gap, whereas the ionization levels of V_{As} are in the upper half of the gap. We observe two ionization processes of a monovacancy in

the upper part of the energy gap close to the conduction band. Hence, it is straightforward to relate the transitions in the positron-lifetime spectra to changes in the As vacancy. Supporting this argument, positron trapping at native vacancy defects has never been observed in any position of the Fermi level in p-type material, where the As vacancy should be positive and thus repulsive to positrons according to theoretical calculations.[26–28] We can thus conclude that the native monovacancy present in GaAs is V_{As}. This interpretation is supported also by our earlier experiments in as-grown or electron-irradiated GaAs.[2,8] Unfortunately, positron lifetime does not indicate whether the As vacancies are isolated or associated to other point defects like impurities and antisites.

According to theoretical calculations, positrons get trapped at neutral or negative monovacancies, but not at vacancies which have a positive charge.[11] The order of magnitude of the changes in the trapping coefficient μ resulting from a change of the monovacancy charge state has also been estimated.[11] Roughly, a charge transition $2- \rightarrow 1-$ decreases the trapping coefficient at room temperature by a factor of 3 and a charge transition $1- \rightarrow 0$ by a factor of 6. There is a decrease of more than an order of magnitude in μ, when the monovacancy becomes positive. In our positron experiments, we find a decrease in μ by at least a factor of 30 in the ionization process at 140 meV below the conduction band. In comparison with the theory, it is thus natural to associate this transition to the ionization $0 \rightarrow 1+$ of the monovacancy defect. Above we identified the monovacancy to V_{As}. We can thus conclude that the As vacancy changes its charge to positive when the Fermi level crosses an ionization level at 140 meV below the conduction-band edge. However, we emphasize that if V_{As} is bound to a defect complex, the charge states must be understood as total charges of the whole complex and not as specific states of V_{As} in it.

The ionization process $\tau_2 = 257$ ps$\leftrightarrow$295 ps at $E_C - E_i = 30$ meV takes place closer to the conduction band than the transition $0 \rightarrow 1+$ of V_{As} at $E_C - E_i = 140$ meV. The process thus corresponds to a transition between two more negative states of the monovacancy than singly positive state. Between 30 and 140 meV we see no transitions in the vacancy defects. It is thus natural to identify the transition at 30 meV to the ionization $1- \rightarrow 0$ of the monovacancy. The change of the trapping coefficient in this transition was estimated to be a factor of 6 ± 1 in Sec. VI B 2. This value is in a good agreement with the ratio of the trapping coefficients which has been calculated for modelized single negative and neutral vacancies.[11] Using the simple identification to V_{As}, we can attribute the lifetime transition 257 ps$\leftrightarrow$295 ps in τ_2 to the ionization $V_{As}^{-} \rightarrow V_{As}^{0}$. Again, we point out that if V_{As} is associated to a defect complex, the charge transition observed here reflect ionizations of the whole complex and not necessarily those of V_{As} in it.

We have previously attributed the $\kappa \rightarrow 0$ transition at 140 meV possibly to ionization $V_{As}^{-} \rightarrow V_{As}^{0}$.[2] However, the analysis of the Fermi functions explained in Sec. VI C suggests strongly that the trapping rate κ decreases by more than 1 order of magnitude in the ionization process. The positron-lifetime experiments in Si give also evidence that neutral vacancies can act as efficient positron traps with not very different trapping coefficient at 300 K compared to negative vacancies.[10,22] In our earlier paper[2] we also considered a bistable reaction $V_{Ga} \rightarrow V_{As} + As_{Ga}$ (Ref. 29) as a possible origin of the transition $\tau_2 = 257$ ps$\leftrightarrow$295 ps at 30 meV. On the basis of our new results, this reaction seems to be less likely, because the change in the trapping coefficient should be more than the factor of 6 we estimated in Sec. VI B 2. With the charge state of $3-$ for V_{Ga} (Refs. 26 and 27) and the total charge of 0 for (V_{As}-As_{Ga}) complex, the total charge would change from $3-$ to 0 instead of the change from $1-$ to 0 during the transition $\tau_2 = 257$ ps$\rightarrow$295 ps.

Our lifetime experiments suggest strongly that As vacancy has a neutral and a negative charge state in the upper part of the energy gap. This result is supported by recent theoretical calculations,[27,28] but not those calculations according to which the As vacancy is always in a positive charge state.[26] However, the positions of the ionization levels are not very close to those given by the theory. For example, we find a level of $E_C - E_i = 140$ meV for the $V_{As}^{0} \rightarrow V_{As}^{+}$ reaction, whereas a value of $E_C - E_i = 320$ meV was obtained for the same ionization level in the calculations.[27] However, we feel that the basic disagreement with the theory is not very strong since the same type of charge states for V_{As} are obtained both in calculations and in our experiments. In addition, if the vacancies seen in our experiment are not clean but decorated, the ionization levels can be expected to be different from the levels of isolated monovacancies.

Our ionization levels for V_{As} are close to the values obtained experimentally by DLTS in electron irradiated GaAs.[30,31] In fact, Loualiche *et al.* have suggested that V_{As} may have even a double negative state close to the conduction band.[31] In as-grown material, only a few observations on electron levels close to the conduction band have been reported.[32] Walukiewicz, Lagowski, and Gatos[33] have suggested that there is a shallow donor state at about 20–30 meV below the conduction band, and according to Ref. 32 this state could be associated with the EL2 defect in GaAs. Indications of the 30-meV (Ref. 34) and roughly 120-meV (Ref. 35) electron levels have also been observed in temperature-dependent Hall experiments. Our positron results suggest that these levels are associated to the ionization of As vacancy. We have checked following the same experimental procedure as in semiinsulating GaAs (Ref. 36) that the as-grown vacancies in n-type GaAs do not have the same metastability as EL2.

In the ionization $1- \rightarrow 0$, we find a large change from 257 to 295 ps in the lifetime of positrons trapped at native monovacancies. This large change can only be explained by a strong lattice relaxation at the ionization process. Because positron lifetime depends on the open volume present in the vacancy, the 38-ps lifetime increase in the transition $1- \rightarrow 0$ is a clear sign that the negative configuration of the native monovacancy is inward relaxed compared to the structure of its neutral state. On the basis of theoretical calculations, we can estimate that

the difference in the relaxation is about 10% in the breathing mode.[37] In the simple identification of the monovacancy defect to As vacancy, we can conclude that the state V_{As}^{-} is strongly inward relaxed compared to V_{As}^{0}. This trend is suggested also by the recent self-consistent *ab initio* molecular dynamics calculations.[38]

In conclusion, we have found two ionization levels of monovacancies at 30 and at 140 meV below the conduction band. We attribute the 30-meV level to the ionization $V_{As}^{-} \rightarrow V_{As}^{0}$ and the 140-meV level to $V_{As}^{0} \rightarrow V_{As}^{+}$. Our results show that V_{As}^{-} is strongly inward relaxed compared to V_{As}^{0}.

E. Concentration of As vacancies in as-grown GaAs

For the estimation of the concentration c_d of As vacancies in our n-type GaAs samples, the value of positron trapping coefficient μ_d has to be known [Eq. (3)]. Unfortunately, in semiconductors the exact value of μ_d is still an open question. The theoretical calculations suggest values of 4×10^{14} and 2.5×10^{15} s^{-1} for neutral and negative vacancies, respectively.[11] In electron-irradiated GaAs, we have estimated that $\mu_d > 6\times10^{14}$ s^{-1} for Ga vacancies with a charge of $3-$.[8] In electron-irradiated P-doped Si positron trapping at neutral and negative vacancy-phosphorus pairs have recently been studied.[22] The results indicate that the positron trapping coefficients at 300 K are roughly 2×10^{15} s^{-1} and 1×10^{15} s^{-1} at the negative and neutral states of (V-P) pairs, respectively.[22] In electron-irradiated Si, positron trapping coefficients of 3.5×10^{15} and 1×10^{15} s^{-1} have also been estimated for negative and neutral divacancies, respectively.[39] Both experimental and theoretical results thus suggest a value of typically $\mu_d = 2\times10^{15}$ s^{-1} for positron-trapping coefficient at negative vacancies at 300 K.

In the samples studied in this work, the trapping rate κ at vacancies can be accurately calculated at 300 K in highly n-type GaAs (Si: 2.0×10^{18}). In this sample positron trapping is observed at only one charge state of the native vacancy, which is V_{As}^{-} according to our identification. The average lifetime at 300 K in this sample is $\tau_{av}=240$ ps (see Table I), which gives a trapping rate of $\kappa = 2.3$ ns^{-1} [Eq. (7)]. With a trapping coefficient of $\mu_d = 2\times10^{15}$ s^{-1}, we get a vacancy concentration of $c_d = 5\times10^{16}$ cm^{-3}. This value is slightly smaller than our earlier estimates of 2×10^{17} cm^{-3},[2] but it is closer to the point-defect concentrations generally believed to exist in as-grown GaAs.[32] In summary, we conclude that positrons detect vacancies typically at concentrations $(5-10)\times10^{16}$ cm^{-3} in n-type GaAs.

VII. CONCLUSIONS

We have investigated systematically by positron-lifetime experiments the properties of native vacancies in as-grown GaAs. Especially, the ionization processes of vacancies were studied by measurements as a function of temperature at 10–600 K in n-type samples with carrier concentrations of $n = 10^{15}-10^{18}$ cm^{-3}. We report also on experiments in p-type samples with $p = 5\times10^{16}$ to 2×10^{18} cm^{-3}. In contrast to n-type GaAs, no signs of native vacancies were observed in p-GaAs.

In n-type GaAs, two types of monovacancies were found with positron lifetimes of 257 ± 3 and 295 ± 3 ps, respectively. The existence of the two configurations can be related to the position of the Fermi level in the energy gap in all samples. The transition between the two types of monovacancies takes place when the Fermi level crosses electron level in the gap at $E_C - 30$ meV. Moreover, the positron trapping rate at a monovacancy with the lifetime of 295 ps is observed to decrease strongly toward zero, when the Fermi level crosses another electron level at $E_C - 140$ meV

We associate the observed Fermi-level-controlled transitions to ionization processes of native monovacancy defects. The monovacancies may be isolated or bound to a defect complex. At $E_C - 140$ meV, the defects involving monovacancies are ionized from neutral to positive, whereas at $E_c - 30$ meV they exhibit a charge transition $1- \rightarrow 0$. We attribute the monovacancies to V_{As}, and hence the ionization processes to $V_{As}^{-} \rightarrow V_{As}^{0}$ ($E_C - 30$ meV) and $V_{As}^{0} \rightarrow V_{As}^{+}$ ($E_C - 140$ meV), respectively. The large lifetime change from 257 to 295 ps in the ionization $V_{As}^{-} \rightarrow V_{As}^{0}$ indicates further that the negative configuration of the native As vacancy is strongly inward relaxed compared to neutral V_{As}. If the monovacancy is part of a defect complex, the charge states given above should be understood as the total charges of the complex.

The present results thus show that all aspects of positron trapping in n-type Si or Sn-doped GaAs can be related to the position of the Fermi level in the energy gap in a large variety of sample doping levels and measurement temperatures. Furthermore, they show that positron-lifetime experiments can be used to get information on the different charges of vacancies and their ionization levels in the energy gap. In comparison with theoretical calculations, the changes in the positron lifetimes can also be used to characterize the lattice relaxations induced by the vacancy ionization process.

ACKNOWLEDGMENT

The authors acknowledge the help of R. Krause in the experiments.

[1] G. Dlubek and R. Krause, Phys. Status Solidi A **102**, 443 (1987).

[2] C. Corbel, M. Stucky, P. Hautojärvi, K. Saarinen, and P. Moser, Phys. Rev. B **38**, 8192 (1988).

[3] S. Dannefaer, D. P. Kerr, and B. G. Hogg, Phys. Rev. B **30**, 3355 (1984); S. Dannefaer and D. P. Kerr, J. Appl. Phys. **60**, 591 (1986).

[4] *Positrons in Solids,* Vol. 12 of *Topics in Current Physics,* edited by P. Hautojärvi (Springer, Heidelberg, 1979).

[5] *Positron Solid State Physics,* edited by W. Brandt and A. Du-

pasquier (North-Holland, Amsterdam, 1983).
[6]K. Saarinen, P. Hautojärvi, A. Vehanen, G. Dlubek, and R. Krause, Phys. Rev. B **39**, 5287 (1989).
[7]S. Dannefaer, P. Mascher, and D. Kerr, in *Positron Annihilation,* edited by L. Dorikens-Vanpraet, M. Dorikens, and D. Segers (World Scientific, Singapore, 1989), p. 714.
[8]C. Corbel, F. Pierre, P. Hautojärvi, K. Saarinen, and P. Moser, Phys. Rev. B **41**, 10 632 (1990).
[9]C. Corbel, F. Pierre, K. Saarinen, P. Hautojärvi, and P. Moser (unpublished).
[10]J. Mäkinen, C. Corbel, P. Hautojärvi, P. Moser, and F. Pierre, Phys. Rev. B **39**, 10 162 (1989).
[11]M. J. Puska, C. Corbel, and R. M. Nieminen, Phys. Rev. B **41**, 9980 (1990).
[12]R. N. West, in *Positrons in Solids* (Ref. 4), p. 89.
[13]J. Bourgoin and M. Lannoo, *Point Defects in Semiconductors II* (Springer, Heidelberg, 1983).
[14]M. J. Puska, J. Phys. Condens. Matter **3**, 3455 (1991); M. J. Puska, O. Jepsen, O. Gunnarsson, and R. M. Nieminen, Phys. Rev. B **34**, 2695 (1986).
[15]*Zahlenwerte und Funktionen aus Naturwissenschaften und Technik, Landolt-Börnstein,* New Series, Group X, Vol. 22 (Springer, Heidelberg, 1989).
[16]C. Corbel, F. Pierre, P. Hautojärvi, K. Saarinen, and P. Moser, in *Defects in Semiconductors,* Vols. 38–41 of Materials Science Forum, edited by G. Ferenczi (Trans Tech, Aedermannsdorf, 1989), p. 791.
[17]C. Corbel, P. Moser, and M. Stucky, Ann. Chim. (Paris) **8**, 733 (1985).
[18]M. J. Puska, O. Jepsen, O. Gunnarsson, and R. M. Nieminen, Phys. Rev. B **34**, 2695 (1986).
[19]M. J. Puska and C. Corbel, Phys. Rev. B **38**, 9874 (1988).
[20]P. Hautojärvi, P. Moser, M. Stucky, C. Corbel, and F. Plazaola, Appl. Phys. Lett. **48**, 809 (1986).
[21]R. Würschum, W. Bauer, K. Maier, A. Seeger, and H.-E. Schaefer, J. Phys. Condens. Matter **1**, SA33 (1989).
[22]J. Mäkinen, C. Corbel, P. Hautojärvi, and K. Saarinen (unpublished).
[23]J. S. Blakemore, J. Appl. Phys. **53**, R123 (1982).
[24]S. M. Sze, *Physics of Semiconductor Devices* (Wiley, New York, 1981).
[25]N. F. Mott, *Metal-Insulator Transitions* (Taylor and Francis, London, 1974).
[26]G. A. Baraff and M. Schlüter, Phys. Rev. Lett. **55**, 1327 (1985).
[27]M. J. Puska, J. Phys. Condens. Matter **1**, 7347 (1989).
[28]H. Xu and W. Lindefelt, Phys. Rev. B **41**, 5975 (1990).
[29]G. A. Baraff and M. Schlüter, Phys. Rev. Lett. **55**, 2340 (1985); H. J. von Bardeleben, A. Miret, and J. C. Bourgoin, in *Defects in Semiconductors,* Vols. 10–12 of Materials Science Forum, edited by H. J. von Bardeleben (Trans-Tech, Aedermannsdorf, 1986), p. 299.
[30]D. Pons and J. C. Bourgoin, J. Phys. C **18**, 3829 (1985).
[31]S. Loualiche, A. Nouailhat, G. Guillot, and M. Lannoo, Phys. Rev. B **30**, 5822 (1984).
[32]J. C. Bourgoin, H. J. von Bardeleben, and D. Stiévenard, J. Appl. Phys. **64**, R65 (1988).
[33]W. Walukiewicz, J. Lagowski, and H. C. Gatos, Appl. Phys. Lett. **43**, 112 (1983).
[34]K. Germanova, V. Donchev, V. Valchev, and Ch. Hardalov, Phys. Status Solidi A **113**, K231 (1989).
[35]R. Krause, A. Polity, G. Dlubek, K. Friedland, R. Rentzsh, W. Siegel, and G. Kühnel, in *Positron Annihilation,* edited by L. Dorikens-Vanpraet, M. Dorikens, and D. Segers (World Scientific, Singapore, 1989), p. 721.
[36]R. Krause, K. Saarinen, P. Hautojärvi, A. Polity, G. Gärtner, and C. Corbel, Phys. Rev. Lett. **65**, 3329 (1990).
[37]S. Mäkinen and M. J. Puska, Phys. Rev. B **40**, 12 523 (1989).
[38]K. Laasonen, R. M. Nieminen, and M. J. Puska (unpublished); K. Laasonen, M. Alatalo, M. J. Puska, and R. M. Nieminen, J. Phys. Condens. Matter **3**, 7217 (1991).
[39]P. Mascher, S. Dannefaer, and D. Kerr, Phys. Rev. B **40**, 11 764 (1989).